
Article:
Mohsenian, V., Filizadeh, R., Ozdemir, Z. et al. (1 more author) (2020) Seismic performance evaluation of deficient steel moment-resisting frames retrofitted by vertical link elements. Structures, 26. pp. 724-736. ISSN 2352-0124

https://doi.org/10.1016/j.istruc.2020.04.043

Seismic Performance Evaluation of Deficient Steel Moment-Resisting Frames Retrofitted by Vertical Link Elements

Vahid Mohsenian[a], Reza Filizadeh[b], Zuhal Ozdemir[c,*], Iman Hajirasouliha[c],

[a] Department of Civil Engineering, University of Science and Culture, Tehran, Iran
[a] Department of Civil Engineering, Sharif University of Technology, Tehran, Iran
[c] Department of Civil and Structural Engineering, University of Sheffield, Sheffield, UK

[*] Corresponding author: z.ozdemir@sheffield.ac.uk

Abstract

In many earthquake prone regions in developing countries, substandard steel moment resisting frame (SMRF) systems pose a profound danger to people and economy in the case of a strong seismic event. Eccentric bracing systems with replaceable vertical links can be utilized as an efficient and practical seismic retrofitting technique to reduce future earthquake damages to such structures. This paper aims, for the first time, to demonstrate the efficiency of eccentric bracing systems with vertical links as a seismic retrofitting technique for the SMRF structures with WCSB and to develop fragility curves for such structures. To achieve this aim, first, the effect of the vertical links on the behaviour of 3, 5 and 7-storey frames are studied through conducting the Nonlinear Static Analyses (NSA) as well as Nonlinear Time History Analyses (NTHA) using the artificial accelerograms compatible with the target design spectrum. The analysis results indicate that, as aimed in the design stage, the seismic damage is only concentrated at the replaceable vertical links and remaining structural members work mainly in the elastic range. In addition, the proposed retrofitting technique considerably improves the performance of the deficient SMRF systems by effectively restricting the displacement response and damage distribution in such structures. Following the NTHA, Incremental Dynamic Analyses (IDA) are performed to develop the seismic fragility curves for the retrofitted SMRF systems. The results indicate that the proposed retrofitting technique significantly reduces the fragility of such systems, and therefore, can provide a simple and efficient method to improve the seismic performance of deficient steel moment resisting frames in seismic regions.

1. Introduction

Substandard structures designed based on old seismic design standards account for a large proportion of the building stock in many large urban areas of developing countries. These buildings generally suffer from problems such as poor detailing and weak columns and strong beams (WCSB), which results in low ductility and limited energy dissipation capacity leading to significant second order effects and soft story mechanism when subjected to strong ground motions. In such cases, the major lateral load-carrying elements of the structures (especially columns) may exhibit extensive damages, as it was observed in the structures designed based on the old generation of Iranian Code of Practice (Standard 2800 [1], [2]) in 2017 Kermanshah earthquake in Iran. This highlights the importance of developing appropriate retrofitting techniques to improve the seismic performance of deficient steel moment resisting frames to reduce the seismic risk under future events.

Eccentrically braced frames (EBFs), originally invented by Roeder and Popov [3], have the ability to combine the energy dissipation capacity of moment resisting frame with the stiffness of a brace frame. Therefore, EBFs can be effectively used for the seismic rehabilitation of steel moment resisting frame (SMRF) systems. The short segment of an EBF is called a “link element”. The characteristics of the link element has a considerable effect on the stiffness, strength and ductility of the EBF system. Previous studies showed that by providing an adequate level of ductility and stiffness in the link elements, they can efficiently

dissipate a large amount of the seismic input energy through plastic deformations under shear and bending [4]. This implies that the link elements in EBFs can be designed to act as a seismic fuse during a seismic event by dissipating seismic energy in a controlled manner.

Popov and his co-workers [5-12] carried out extensive experimental research on EBFs to assess the effect of link length, stiffener spacing and placing of stiffeners on the performance of such systems. The current design criteria provided in seismic design provisions (ANSI/AISC 341-16 [13]) for EBFs are mainly based on their research work. The length of shear link can be represented as $e = \rho\, M_P/V_P$, where ρ is a constant coefficient, and M_p and V_p are the plastic flexural moment and shear capacities of the link, respectively. The link elements with $\rho \leq 1.6$ are called short links and they mainly yield in shear. Previous research undertaken by Roeder and Popov [5,6], Hjelmstad and Popov [8,9], Ghobarah and Ramadan [14], and many others demonstrated the superior performance of EBFs with short links in terms of stiffness, strength and ductility. Links with $1.6 < \rho \leq 3$ are called intermediate links and they undergo yielding in a combination of bending and shear actions. Finally, the behaviour of long links with $\rho > 3$ is dominated by yielding in bending. Due to some architectural advantages (for instance accommodation of large openings), longer links have been used more widely than short links. Intermediate and long links with $\rho > 1.6$ generally exhibited poor performance when they used in a configuration attached to the column, however, a better performance was observed when they placed in between braces [12]. More recently, Daneshmand and Hashemi [15] investigated the seismic performance of intermediate and long links in eccentrically braced frames designed based on ANSI/AISC 360-10 [16] using a series of Finite Element Analysis.

As link elements are designed to act as a seismic fuse during a seismic event, they need to be easily replaceable. In some cases, such as horizontal links, the replacement of these elements can be very costly and time-consuming. In addition, in some certain link sizes and configurations, these elements can undergo complex strain and stress states, which makes them very difficult to analyse and design. The EBF systems with vertical links, originally developed by Seki et al. [17], can eliminate some of the above mentioned drawbacks of conventional EBFs. They can also provide high energy absorption capacity, high ductility and good seismic performance [18]. As a result, the response modification factors up to 8 can be used for seismic design of these systems under DBE and MCE hazard levels [19]. In addition, vertical links do not result in stress concentration or additional deformation in story beam. Research carried out on EBF systems with vertical links showed that the seismic energy acting on such systems can be entirely dissipated by the vertical links while the remaining structural elements (i.e. beams, columns and braces) remain in elastic or near elastic state [4, 20]. Therefore, the vertical links can be designed as replaceable elements equipped with high ductility and energy absorption capacity. As a result, EBFs with vertical links offer an attractive solution for seismic rehabilitation and retrofitting of the existing and deficient structures due to their simple working mechanisms, replaceability and convenient implementation.

Similar to EBF systems with horizontal links, the link length has substantial effect on the response of the EBF systems with vertical links. An increase in the link length above a certain value may cause brittle fractures due to multi-axial stresses [21], while a reduction in critical load, rotation capacity and stiffness of the EBF systems can be also expected [22]. On the basis of the studies conducted by Zahrai and Parsa [23], if sufficient bearing area is provided for the vertical links, even in case of reduction in flange width, the resulted hysteretic loops will be adequately wide and stable showing a good energy dissipation capacity. The shaking table tests carried out on high-strength SMRF combined with conventional steel EBF with vertical shear links showed good cyclic behavior and high energy dissipation and lateral load-carrying capacity of these systems [24]. The use of mild steel in vertical links prevents the occurrence of local buckling and hence improves the energy dissipation capacity of the EBFs when compared with vertical links made from hard steel [25]. Cyclic tests carried out on half-scale high-strength eccentrically braced steel frames with normal-strength vertical steel links demonstrated that EBF systems with shear yielding vertical link outperformed EBF systems with flexural yielding vertical links [26]. The use of shape memory alloy in vertical links improves the ductility, lateral stiffness and strength as well as self-centering capability of the buildings, while also considerably reduces the inter-storey and residual drifts [27]. Experiments conducted

by Shayanfar et al. [28] on partially-encased composite steel vertical link elements demonstrated that the presence of stiffeners and concrete in the link can delay the occurrence of the shear buckling in the link, and consequently, play an important role in ductility and energy dissipation enhancement of the EBF systems. Other empirical and analytical studies carried out on the EBF systems with vertical links (e.g. Bouwkamp et al [29]; Vetr et al. [30]) showed that the ultimate shear strength of the link is generally up to 2.2 times greater than its nominal shear yielding value.

EBFs with double vertical links, as originally developed by Fehling et al. [31], can also provide a good solution for the rehabilitation of deficient structures, particularly when a single large size vertical link cannot be accommodated onto beams due to space limitations and/or when large shear forces are transferred to the beams. Numerical studies [32-33] and experimental work [34] carried out on such systems exhibited the stable hysteretic curves of double links with wider loops, resulting in better energy dissipation capacity during an earthquake event compared to the systems with single vertical links. Zahrai and Mahroozadeh [35] conducted a number of experimental tests on EBF systems with single and double links and found that rotation angle of the link element ranges from 0.128 to 0.156 rad (radian) prior to the fracture initiation. Moreover, it was found that the equivalent viscous damping ratios vary between 26.7 and 30.6% while the response modification factors (R) of the EBF systems range between 7.15 and 10.65. Rahnavard et al. [33] showed that the increase in the distance between the double vertical links improves the general behaviour of the EBFs and reduces the detrimental effects of the concrete slab on the behaviour of the frame and shear links. Results of reliability analysis carried out on steel frames equipped with EBFs with double links also demonstrated that the application of response modification factor up to 8 can generally provide an acceptable seismic reliability under moderate to high seismic scenarios [36].

The literature review presented in this paper reveals that, there is not any analytical or empirical studies conducted on the EBF systems to evaluate the efficiency of vertical links in rehabilitation and retrofitting of the SMRF systems with WCSB. In addition, the fragility curves for the EBF systems with the vertical links has not been developed so far. Therefore, in this study, the design process of the EBF systems with vertical links is described in the framework of reliability analysis studies. Then, the seismic response of such systems are investigated thoroughly by performing a number of advanced analysis techniques (NSA, NTHA and IDA) on the case study buildings. The results show that the EBF systems with vertical links benefit from high seismic reliability as well as design flexibility, rapid installation and ease of replace-ability following an earthquake. It is also observed that as a retrofitting approach, they can provide sufficient strength and ductility to the deficient structure.

2. Case Studies

A series of SMRFs with WCSB are analyzed as case study examples to investigate the effect of EBF systems with vertical links on the seismic performance of such buildings. 3, 5 and 7-storey bare frames are designed based on the old generation of the Iranian Code of Practice for Seismic Resistant Design of Buildings (Standard 2800) [1] published in 1988. Unlike current seismic design guidelines (such ANSI/AISC 360-10 [16] and ASCE/SEI 7-10 [37]), this old standard does not enforce the adoption of strong-columns weak-beams. Also the structures designed based on this standard generally suffer from poor connection detailing which limits their deformation capacity. This highlights the need for seismic retrofitting of such systems.

The selected structural systems are assumed to be symmetrical in plan and elevation, and therefore, the 3D torsional effects can be practically ignored. In this study, each 2D frame was designed and modelled based on the projected loads as presented in Figure 1. In all models, frame geometry and column and beam sections are designed symmetric with respect the z-axis. All frames have a span length of 5 m and story height of 3.2 m. For all frames, dead load,Q_D, and live load, Q_L, are applied uniformly at all levels. Figure 1 shows the geometry, and dead and live load arrangements of the case study buildings.

The case study buildings are assumed to be located in a highly seismic area in Iran. For high seismic hazard zones, Iranian Code of Practice for Seismic Resistant Design of Buildings [2] recommends a peak ground

acceleration (PGA) of 0.35 g for a return period of 475 years (Design Basis Earthquake-DBE). The structures are assumed to be founded on soil type "III" ($175\ \mathrm{m/s} \leq V_S \leq 375\ \mathrm{m/s}$) according to soil classification provided by the Iranian Seismic Design Code [2]. Using PGA value and soil type, a design spectrum is created according to Iranian Seismic Code of Practice for Seismic Resistant Design of Buildings [2] for the analysis of the case study buildings. The column and beam dimensions are provided in Table 1 according to element labels given in Figure 1. Moreover, it is assumed that the structures are made of steel (ST37) with yielding stress of 240 MPa and Poisson's ratio of 0.3.

The hollow block flooring system used in the case study buildings is considered to act as a rigid diaphragm, while the composite action provided by the floor system is not considered in the numerical models. It should be mentioned that the effect of the composite action on the seismic performance of steel moment resisting frames has been investigated by Elkady and Lingnos [38]. The results of their study indicate that, on average, the composite action may improve the seismic performance of SMRFs, while it may also trigger collapse mechanisms at bottom storey levels.

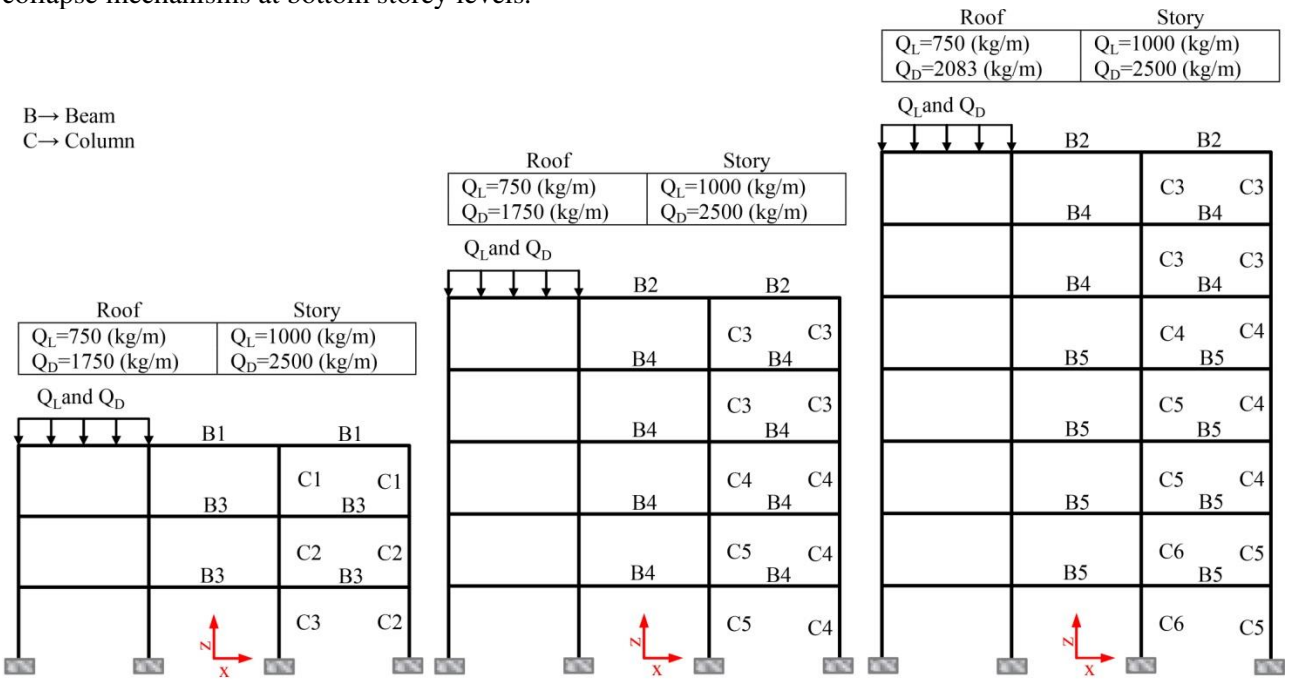

Figure 1- Geometry, and dead and live load arrangements of the case study buildings

Table 1: Section sizes of the structural members for the 3-Storey, 5-Storey and 7-Storey bare frame structures (units: mm)

ID	Section	ID	Section	ID	Section
C1	BOX(150×150×10)	C5	BOX(250×250×20)	B3	2PL200×15& PL270×8
C2	BOX(200×200×12)	C6	BOX(250×250×25)	B4	2PL200×2& PL260×8
C3	BOX(200×200×15)	B1	2PL150×12 & PL276×8	B5	2PL200×2& PL310×10
C4	BOX(200×200×20)	B2	2PL150×15 & PL270×8		

2.1. Nonlinear Modelling Assumptions for Columns and Beams

In this study, PERFORM-3D software [39] was used for pushover and nonlinear dynamic analysis of the frames. Moment and axial-moment interaction hinges were assigned to the two ends of the beam and column

elements, respectively (i.e. critical points prone to the formation of plastic hinges). To define the non-linear behaviour of beams and columns, the generalized load-displacement response curve shown in Figure 2 was adopted in accordance with ASCE/SEI 41-17 [40]. The P-Delta effects were also considered in the analyses using PERFORM-3D [39].

It should be mentioned that there are other models in the literature to simulate the cyclic behaviour of steel members. For example, based on a large database of experimental data of steel components, Lignos and Krawinkler [41] proposed empirical relationships for more accurate modelling of the strength and stiffness deterioration of steel members under cyclic loading. However, the nonlinear model used in this study is widely accepted for practical applications.

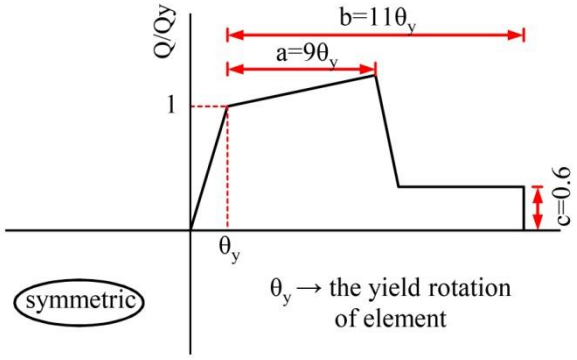

Figure 2- Force-deformation curve for beams and columns (adopted from ASCE/SEI 41-17 [40])

2.2. Nonlinear Modelling Assumptions for Braces

In the numerical models of case study buildings, bar elements are utilized to simulate the behaviour of braces. In the eccentric bracing systems with vertical links, both ends of braces are pinned, therefore the earthquake-induced energy is absorbed through the formation of the axial hinges. For hinged braced elements, brace axial deformations at the expected buckling load, Δ_C, and at the tensile yield force Δ_t are taken as criteria for ductility and nonlinear behaviour according to ASCE/SEI 41-17 [40]. Axial deformations, Δ, of these elements can be computed as follows:

$$\Delta = \frac{F\,L}{E\,A} \tag{1}$$

where F represent brace element force, L is the free length of a brace member, E is elastic modulus of material that braces are made of, and A is the cross-sectional area of a brace member. Tensile, Δ_t, and compressive deformations, Δ_C, of brace members can be computed by replacing F in Eq. (1) with the expected strength of the brace under tension, T_{CE} and with the lower limit of strength under compression P_{CL}, respectively. Behavioral characteristics of the braces as well as their acceptance criteria in the nonlinear range are defined based on the generalized force-deformation curve recommended by ASCE/SEI 41-17 [40] as depicted in Figure 3 considering the failure mode and properties of brace sections.

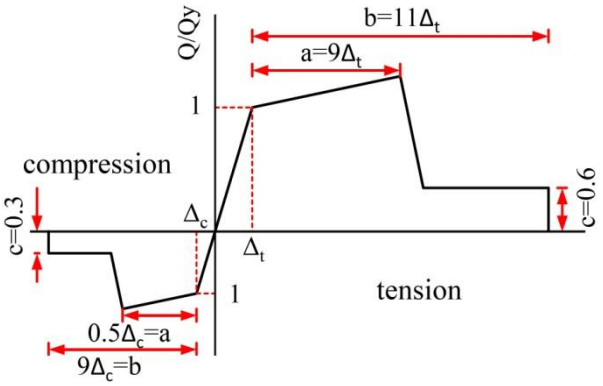

Figure 3- Force-deformation curve adopted for the brace elements in tension and compression ASCE/SEI 41-17 [40]

The layout of the braces and vertical links for the case study structures are shown in Figure 4 and the section sizes selected for these elements at the end of design stage are presented in Table 2.

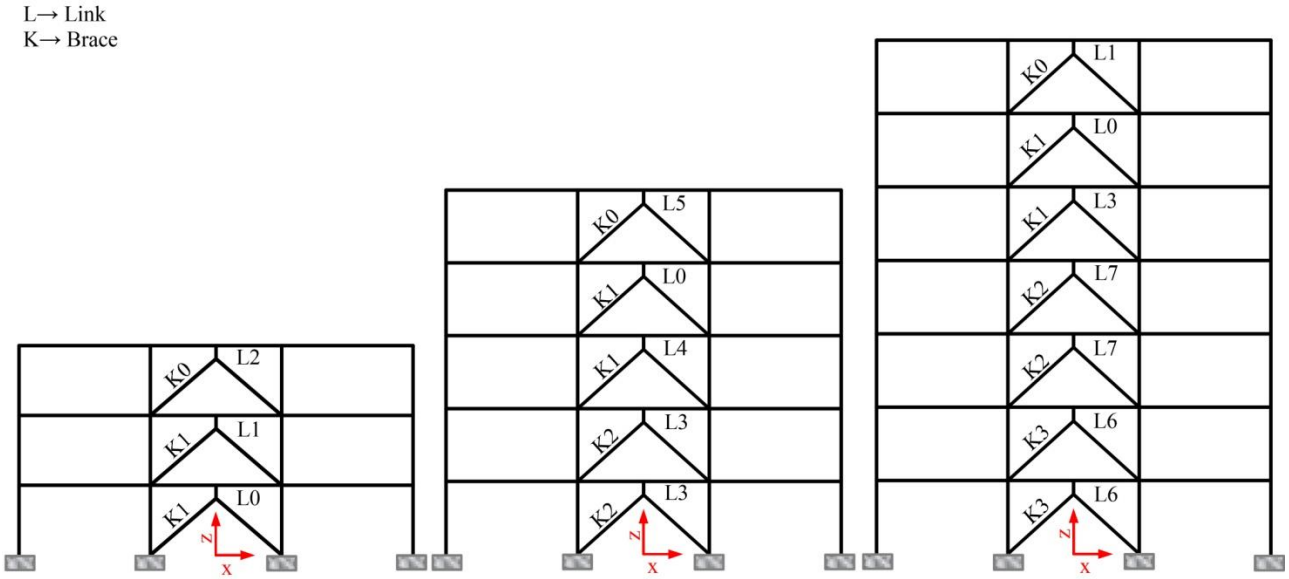

Figure 4- Layout of the braces and vertical links for the retrofitted case study structures

Table 2- Design results for braces and vertical links (units: mm)

ID	Section	ID	Section	ID	Section
K0	2UNP100	L0	IPE 270	L4	IPE 300
K1	2UNP120	L1	IPE 240	L5	IPE 200
K2	2UNP140	L2	IPE 160	L6	IPE 400
K3	2UNP160	L3	IPE 330	L7	IPE 360

2.3. Nonlinear Modelling Assumptions for Vertical Links

The seismic design codes (such as ANSI/AISC 341-16 [13]) limit the length of shear link e according to following equation to assure that shear failure precedes bending failure:

$$e \leq 1.6\, M_p/V_p \tag{2}$$

where M_p and V_p are the plastic flexural moment and shear capacities of a link, respectively, which are computed using the following equations:

$$M_P = Z\, F_y \tag{3}$$

$$V_P = 0.6\, F_y\, A_{lw} \tag{4}$$

where Z is plastic section modulus of the link, F_y is the specified minimum yield strength of the material and A_{lw} is the link web area.

In this work, vertical links are designed in a way to act as sacrificial fuses under the DBE. Therefore, they are allowed to yield earlier than the other members. In each floor, the links are designed to withstand only 50% of the story force to ensure they exhibit yielding under the design earthquake. Therefore, the length of these elements is taken equal to 200 mm [22] to ensure that shear yielding takes place in the vertical links and energy dissipation capacity of vertical links are enhanced. The shear link length of 200 mm is less than that of obtained from Equation (2). This proves that the links will definitely undergo shear yielding. The shear capacity of the link element V_P is calculated based on the detailed FE models (see Figure 5) and has been taken into account to define the load-displacement curve of the link elements. It is worth noting that shear capacities of the elements are in good agreement with the values obtained from Equation (4).

In addition to the link length, the link rotation angle has great significance on the behavior of EBF systems. γ is defined as the angle between the link and the beam outside of the link, when total drift of the structure is equal to the design story drift. For shear links defined with Equation (2), the rotation angle of the link is limited to 0.08 rad for links of length $1.6\, M_p/V_p$ or less and 0.02 rad for links of length $2.6\, M_p/V_p$ or greater according to ANSI/AISC 341-16 [13]. In this paper, γ is limited to 0.1 rad (the strain corresponding to the ultimate stress limit in the links) in the event of DBE.

To develop capacity curves for vertical link elements, Nonlinear Finite Element Analyses (NFEA) are performed on such elements listed in Table 2 in accordance with the AISC Seismic standards using ABAQUS software [42]. Figure 5 depicts Von Mises stress field developed on a vertical link element. As one can observe from this figure, the stress in web is always higher than the stress developed in the flanges. This observation verifies the accuracy of nonlinear modelling of the links and also satisfies the assumption of shear yielding in them. Using the rotation angle observed from FEA results, four damage limit states are defined for the vertical links as shown in Table 3. The developed capacity curves are transferred into a bi-linear elastic-perfectly plastic form to perform nonlinear time history analysis of EBF systems with vertical links using the PERFORM-3D software [39].

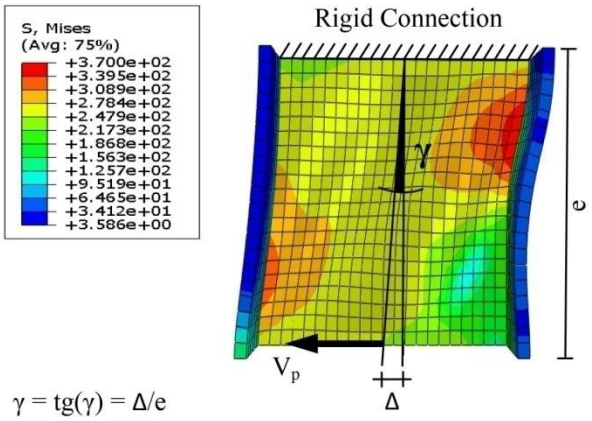

Figure 5- Stress field developed on a vertical link element

Table 3- Damage limit states for the vertical links

Damage Limit States			
(1)	(2)	(3)	(4)
$\gamma=\gamma_y=0.0024$(rad)	$\gamma=0.05$(rad)	$\gamma=0.08$(rad)	$\gamma=0.1$(rad)
$F_y=240$ (MPa)	$F_y<\sigma< F_u$	$F_y<\sigma< F_u$	$F_u=370$ (MPa)

In the PERFORM-3D model of the case study structures, vertical links are defined as "column" elements with linear behaviour and concentrated "shear" hinges. Column elements are assumed to be fixed at the base.

3. Inelastic Dynamic Response

Before performing the Nonlinear Time History Analysis (NTHA), Eigen-value Analyses are conducted on both bare frame (Figure 1) and retrofitted (Figure 4) case study buildings to find modal characteristics of the such structures. For both Eigen-value analysis and NTHA, Gravity loads, Q_G, acting on the systems are computed following the provisions of the ASCE/SEI 41-17 [40]:

$$Q_G = 1.1\,[Q_D + 0.2\,Q_L] \tag{5}$$

The results of the Eigen-value Analysis for both bare frames and retrofitted systems are given in Table 4 in terms of the periods, T, and effective mass participation factors, M, for the first three modes. The results indicate the remarkable impact of the eccentric bracings with vertical link on the modal characteristics of the case study buildings. As one can note from these results, the addition of the EBF systems with vertical links to the bare frames reduce the period of first translational mode by 62.5%, 61.16% and 56.7% for 3, 5 and 7-storey frames, respectively. Based on this, it can be confidently concluded that this technique is capable of significantly increasing the lateral stiffness of the structures. After retrofitting, the translational effective mass in the first mode increased in the all three case study buildings (4.55% for the 3-storey building and nearly 2% for the 5-storey and 7-storey buildings). As the period of first mode is less than 1 s and effective mass participation factor for the first mode is higher than 75%, for the case study buildings the assumption of inverted triangular distribution of earthquake loads along the height of the structures is better satisfied for the retrofitted systems than the bare frames.

Table 4- Periods (T) and Translational Effective Mass Participation Factors (M) for the bare frames (Figure 1) and the retrofitted frames (Figure 4)

Mode No.	3 storey frame				5 storey frame				7 storey frame			
	Original		Retrofitted		Original		Retrofitted		Original		Retrofitted	
	T (s)	M (%)	T (s)	M (%)	T (s)	M (%)	T (s)	M (%)	T (s)	M (%)	T (s)	M (%)
1	0.80	83.49	0.30	87.30	1.03	81.70	0.40	83.31	1.27	78.7	0.55	80.82
2	0.34	12.04	0.11	10.39	0.36	11.62	0.14	10.83	0.47	12.1	0.19	11.23
3	0.18	4.47	0.07	2.31	0.22	3.71	0.08	3.10	0.27	4.23	0.11	3.84

3.1. Nonlinear Time-History Analysis (NTHA)

The accelerograms used in the Nonlinear Time History Analysis (NTHA) should reflect the characteristics of the earthquake source, faulting mechanism, fault distance, magnitude and site effects. In this work, twelve far-field accelerograms are selected from PEER database [43] considering the consistency between the site conditions for the case study buildings and for the sites where earthquakes were recorded. While there are different methods for scaling the input earthquake records, including the methods suggested by Baker [44] and Haselton et al. [45], in this study the selected earthquake records listed in Table 5 are scaled using the wavelet transform function [46] to generate design spectrum compatible artificial earthquake records. In Figure 6, the spectra of the artificially generated earthquake records are compared with the target design spectrum, which is defined in Section 2. There is a good match between spectral ordinates of the artificial records and target spectrum over the all period ranges.

Table 5- The real earthquake records used in the generation of artificial accelerograms

Record	Earthquake & Year	Station	R[a](km)	Component	Mw	PGA(g)
R1	Imperial Valley, 1979	El Centro Array#11	29.4	230	6.5	0.38
R2	Chi Chi(Taiwan), 1999	TAP095	109.01	90	7.6	0.15
R3	Loma Prieta, 1989	CDMG58224	72.2	290	6.9	0.24
R4	Loma Prieta, 1989	CDMG58472	74.26	270	6.9	0.26
R5	Kobe (Japan), 1995	HIK	95.72	0	6.9	0.14
R6	Loma Prieta, 1989	CDMG58223	58.65	0	6.9	0.23
R7	Manjil (Iran), 1990	Qazvin	49.97	336	7.4	0.13
R8	Loma Prieta, 1989	Capitola	27.0	0	7.1	0.53
R9	Landers, 1992	Yermo Fire Station	86.0	270	7.3	0.24
R10	Duzce (Turkey), 1999	Bolu	41.3	90	7.1	0.82
R11	Imperial Valley, 1979	Delta	33.7	352	6.5	0.35
R12	Northridge, 1994	Canyon Country-WLC	26.5	270	6.7	0.48

[a] Closest Distance to Fault Rupture

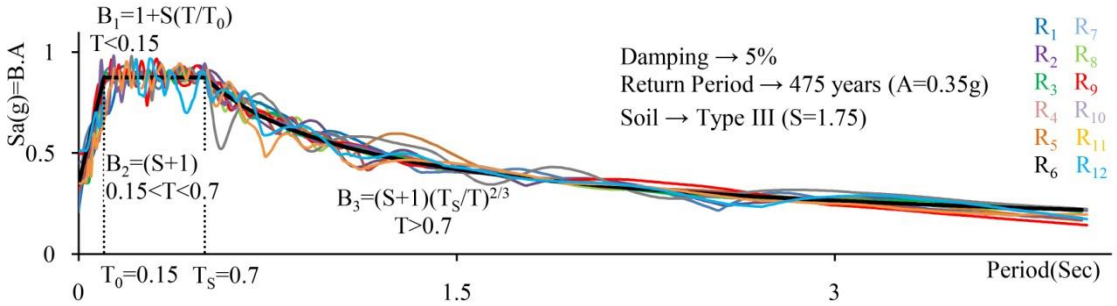

Figure 6- Comparison of the target design spectrum with the response spectra of the artificially generated records

All NTHA results are processed and the outcomes for most critical accelerogram, which yields the maximum dynamic and residuals drifts for the case study buildings are presented in this paper. Figure 7 compares the percentages of energy dissipated by the different group of elements of the bare frame and retrofitted 3-Storey, 5-Storey and 7-Storey case study buildings, when subjected the critical accelerogram. As one can observe from this figure, after retrofitting, the energy dissipation is mainly undertaken by the vertical links. It means that the damage is concentrated in the vertical links, while the other members (i.e. beams, columns and braces) remain elastic under this level of intensity. Notably, a similar behaviour is also observed when the case study buildings are subjected to other records.

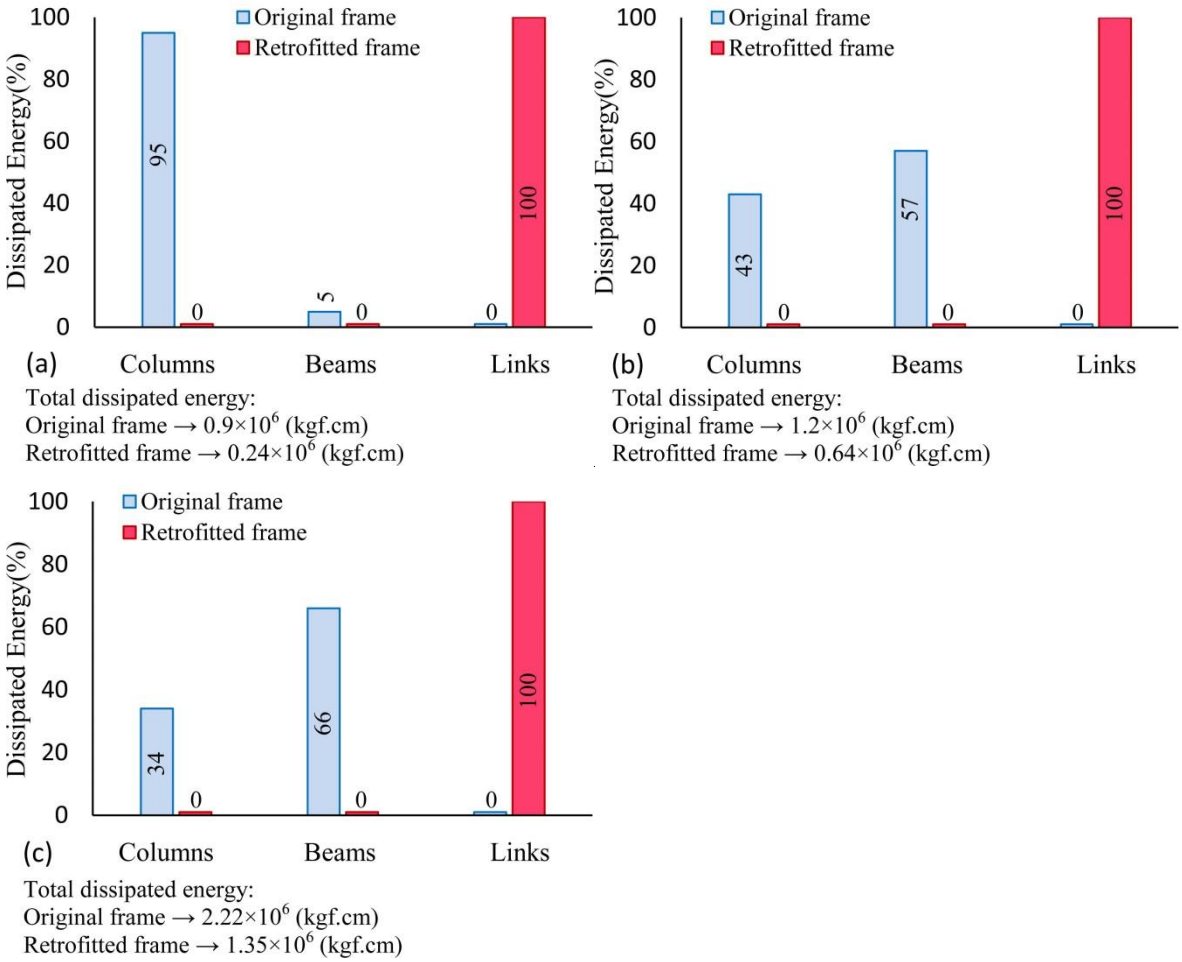

Figure 7- Percentages of the energy dissipation in different element groups of (a) 3-Storey, (b) 5-Storey and (c) 7-Storey case study buildings before and after retrofitting

Figure 8 shows the distribution of the plastic hinges in the 3-Storey, 5-Storey and 7-Storey case study buildings before and after retrofitting when subjected to critical accelerogram. The results indicate that the vertical links have played a major role in restricting the damages. After retrofitting the bare frames, the damages are entirely concentrated in the links. The demand to capacity (D/C) ratios for shear and compressive axial actions in beams and braces of bare frame and retrofitted case study buildings, respectively, are presented in Figure 9. Similarly, the demand to capacity (D/C) ratios for shear and axial actions in the columns of case study buildings before and after retrofitting are given in Figure 10. After retrofitting, the value of plastic shear strain in the vertical links is always less than the limit state corresponding to the ultimate stress in the steel materials (i.e. 0.1 Rad). For the beam and column elements, the maximum plastic rotations for the IO, LS and CP performance levels were assumed to be $1.25\theta_y$, 10 θ_y and 12 θ_y, respectively, where θ_y is the yield rotation of the member. The addition of the shear links reduces the shear demand developed in the beams and columns of all case study buildings. However, the axial forces in the columns located in the braced bays (particularly the lower stories) slightly increase. The maximum compressive axial action in the brace members is still lower than the buckling capacity of these members. Such findings demonstrate the positive effect of the vertical links on the performance of SMRF systems with WCSB.

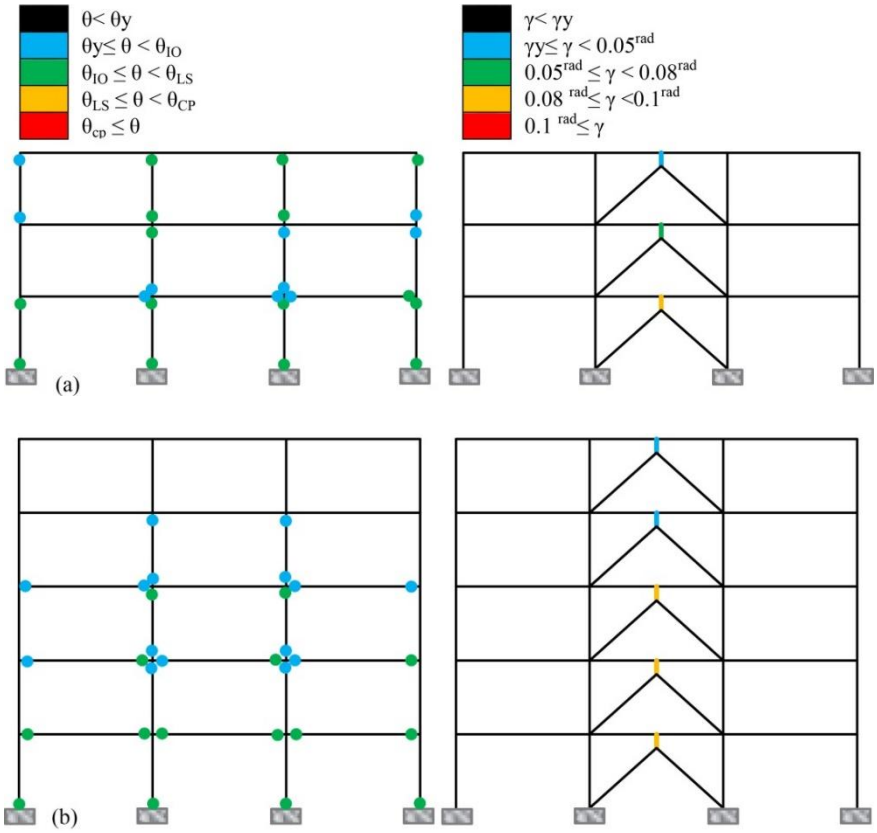

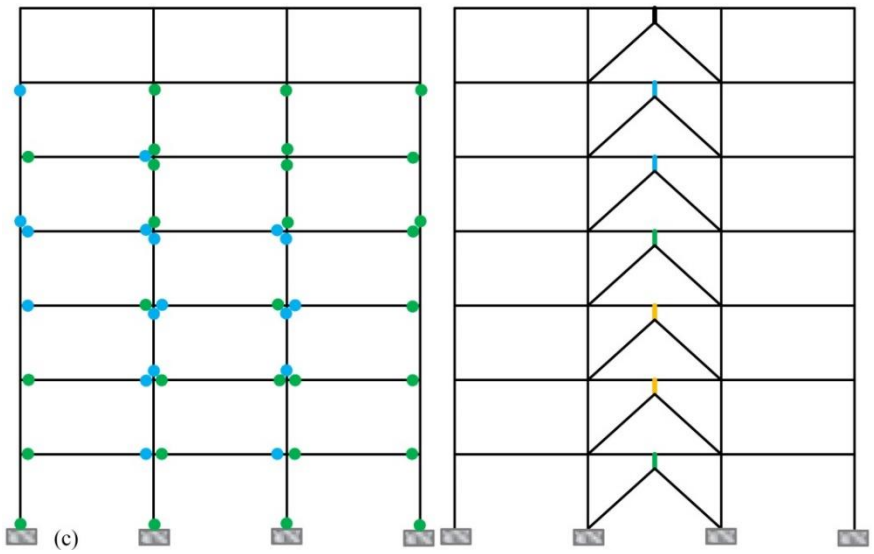

Figure 8: The local performance levels for beams, columns and links and the distribution of the flexural plastic hinges (a) 3-Storey, (b) 5-Storey and (c) 7-Storey case study buildings before and after retrofitting when subjected to the critical accelerogram

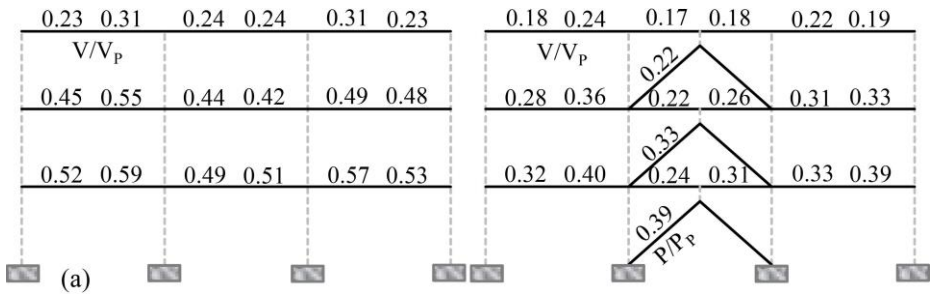

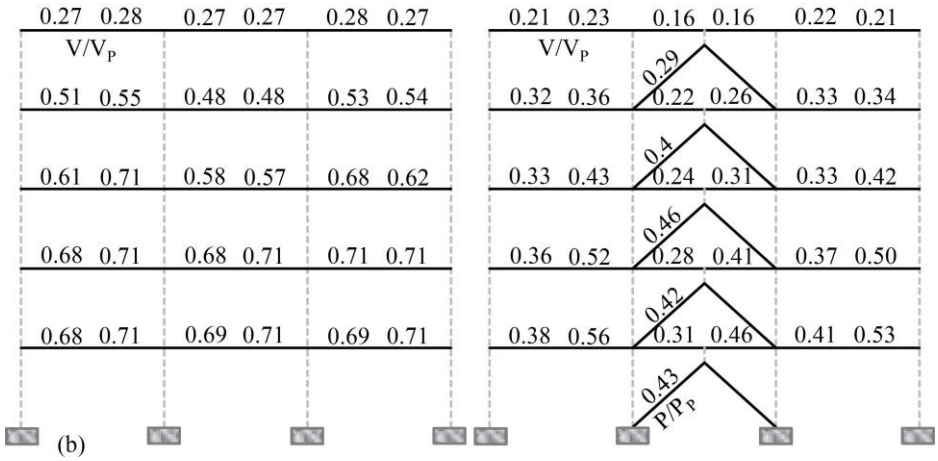

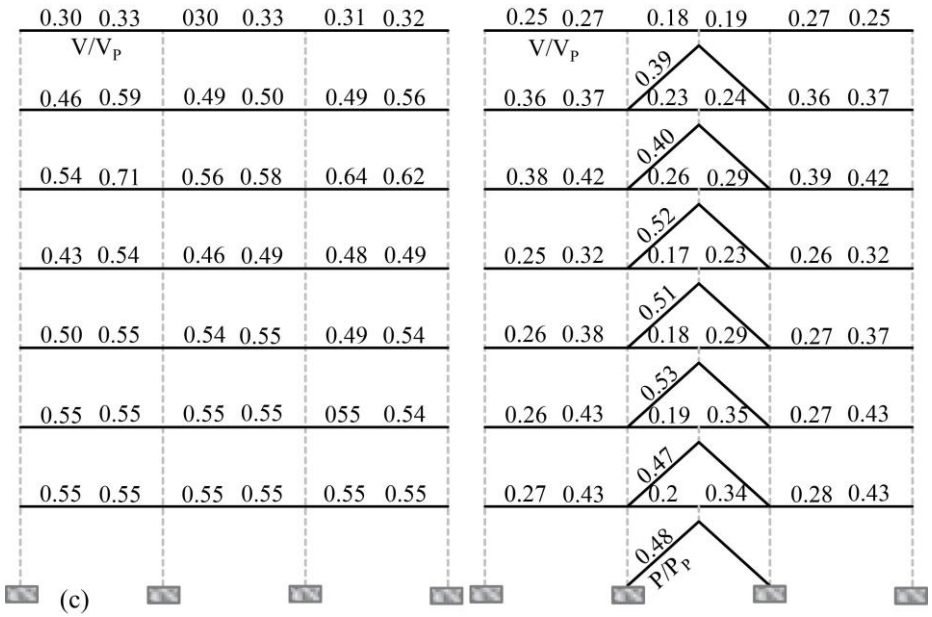

Figure 9- Demand to capacity (D/C) ratios for shear and compressive axial actions in beams and braces, respectively, for (a) 3-Storey, (b) 5-Storey and (c) 7-Storey case study buildings when subjected to the critical accelerogram

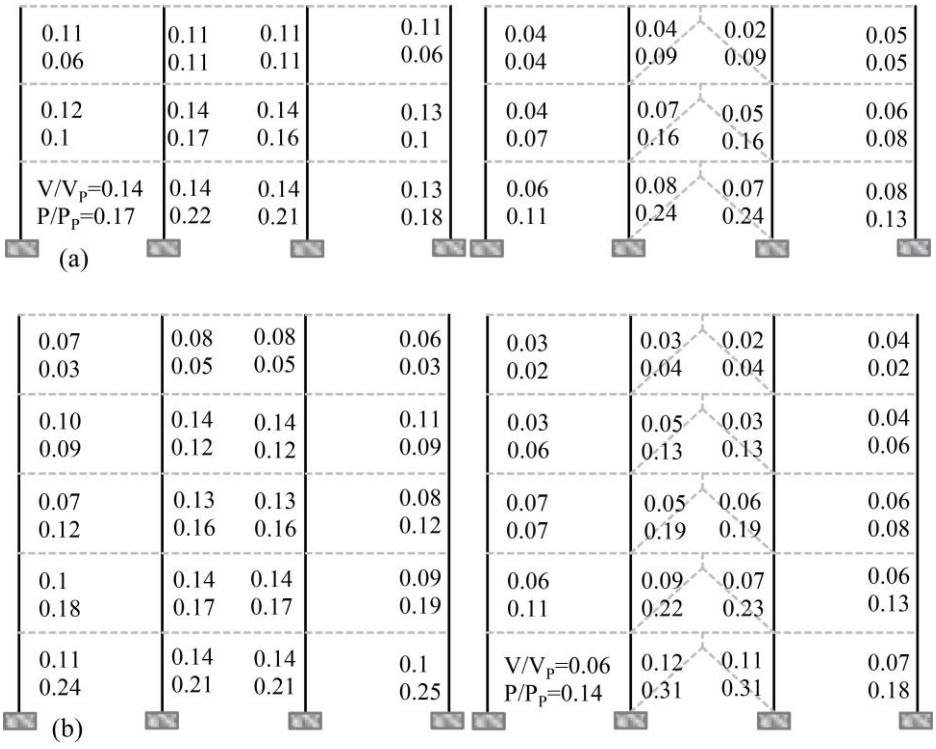

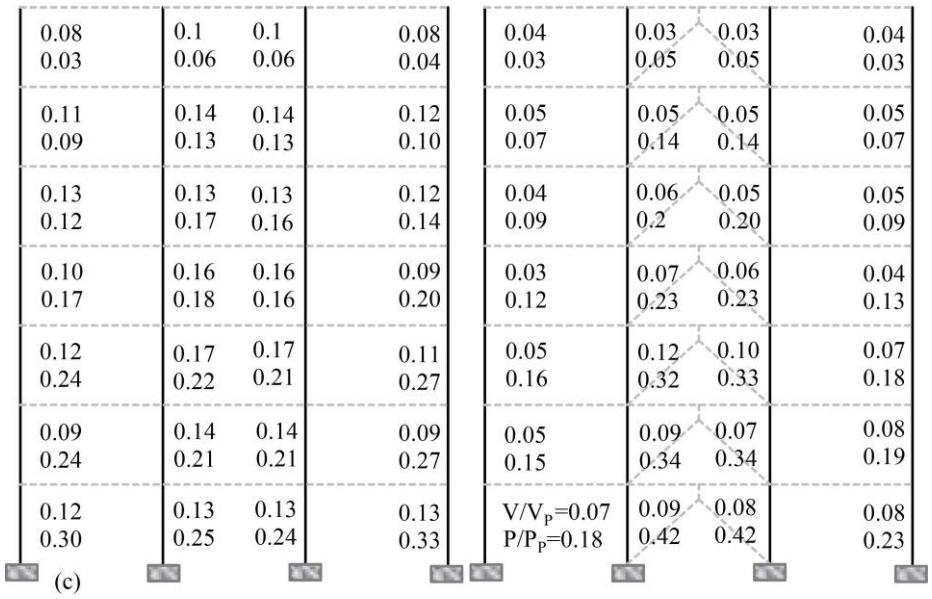

Figure 10- Demand to capacity (D/C) ratio for shear and axial actions of the columns for (a) 3-Storey, (b) 5-Storey and (c) 7-Storey case study buildings before and after retrofitting when subjected to the critical accelerogram

3.2. Nonlinear Static (Pushover) Analysis

A series of nonlinear static analysis (NSA) are carried out on 3-Storey, 5-Storey and 7-Storey bare frame and retrofitted case study buildings. A lateral force distribution pattern, which is consistent with the fundamental mode shapes of the structures, is adopted to represent the distribution of the seismic loads along the height of the structures. Sufficient number of modes, which represents at least 90% of the mass of the structures, are included in the analyses (Table 4). Figure 11 illustrates the lateral load patterns used for the NSA on 3-Storey, 5-Storey and 7-Storey bare and retrofitted frames. The first mode shapes are shown by dotted lines in this figure. In this study, the target drifts used in the pushover analyses are calculated by averaging the maximum drifts (the ratio of roof displacements to the total heights of the structures) obtained from NTHA results for all artificial accelerograms.

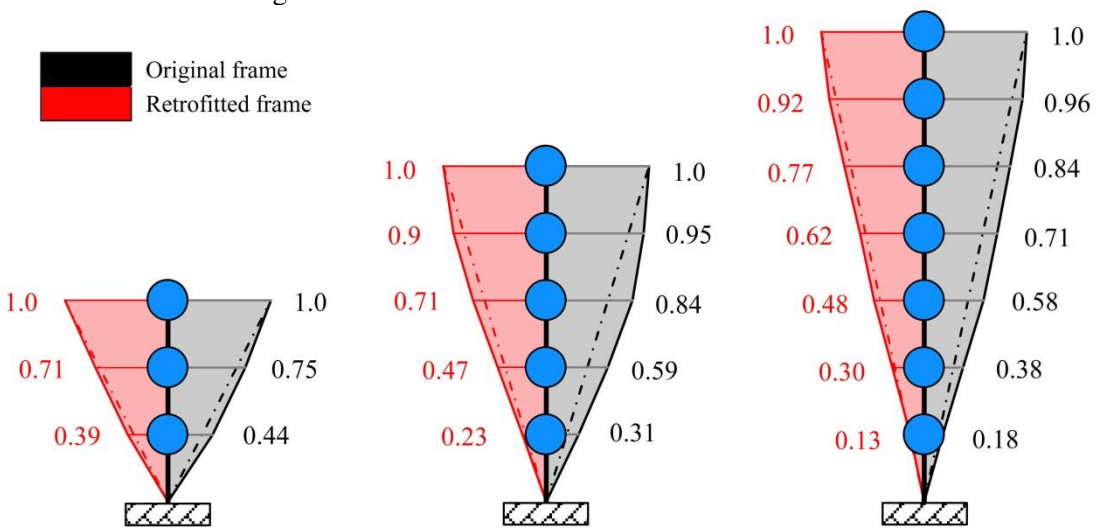

Figure 11- The lateral load patterns used for nonlinear static analysis based on the fundamental mode shapes of the structures before and after retrofitting

In Figure 12, the capacity curves obtained from pushover analyses for the all case study structures are presented in the form of normalized base shear (the ratio of the base shear to the weight of the structure) vs drift curves. Target drifts for both bare frame and retrofitted case study buildings are also shown on the same figure. In addition, the drifts corresponding to performance levels (Immediate Occupancy-IO, Life Safety-LS and Collapse Prevention-CP) defined in ASCE/SEI 41-17 [40] are indicated on this figure. For better comparison, the design base shear (DBS) values for different models are also shown in Figure 12. It can observed from these figures that the proposed retrofitting method considerably enhances the initial stiffness and capacity of the bare frames leading to reduction in the target displacements as achieving high levels of performance. After retrofitting, the abrupt loss of stiffness and capacity does not appear implying the fact that the braces do not buckle in compression and vertical links yield earlier than the other members. In addition, the beginning parts of capacity curves of the retrofitted systems have two successive slopes. This represents a dual load-carrying system with varying levels of ductility and with multi-level energy absorption capability.

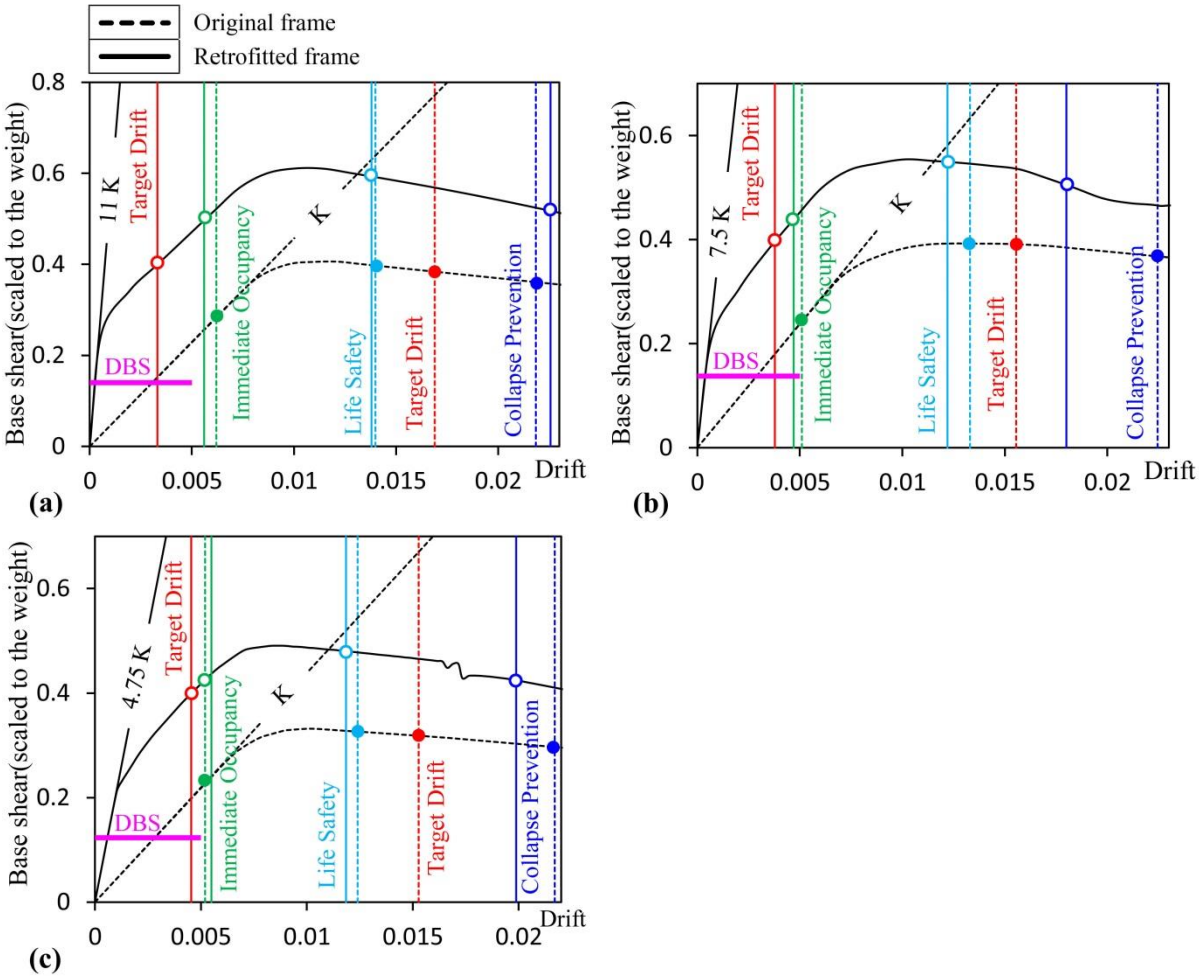

Figure 12- Capacity Curves for (a) the 3-Storey, (b) 5-Storey and (c) 7-Storey bare frame and retrofitted case study buildings

In this section, it is aimed to compare the accuracy of the pushover and time-history analysis methods for assessment of the seismic demands and performance levels in the DBE hazard level. Maximum inter-storey drifts and storey shear forces in both original and retrofitted structures are obtained under the set of 12 earthquake records consistent with the site demand spectrum (see Figure 6), and the mean values are considered as the response corresponding to the DBE hazard level.

Figure 13 shows the comparison of inter-storey drift ratios and storey shear forces obtained from the NTHA and pushover analyses at the target drift levels for (a) the 3-Storey, (b) 5-Storey and (c) 7-Storey bare frame and retrofitted case study buildings. For the retrofitted case study buildings, the NTHA and pushover analysis results are very consistent in terms of both inter storey drift ratios and storey shear forces. As one can observe from this figure that the proposed retrofitting technique significantly enhances the lateral stiffness of the buildings and consequently, control the displacement responses of these structures leading to upgrading the performance levels. The all three SMRF systems with EBF systems with vertical links experience a performance level higher than IO. The NTHA results indicate that the storey shears in retrofitted systems are less those observed in bare frame buildings due to the contribution of vertical link elements in energy dissipation. However, for the retrofitted structures, storey shear forces predicted by the pushover analyses are higher than those obtained by the NTHA. This can be attributed to the static nature of the pushover analysis and its direct relation to the stiffness.

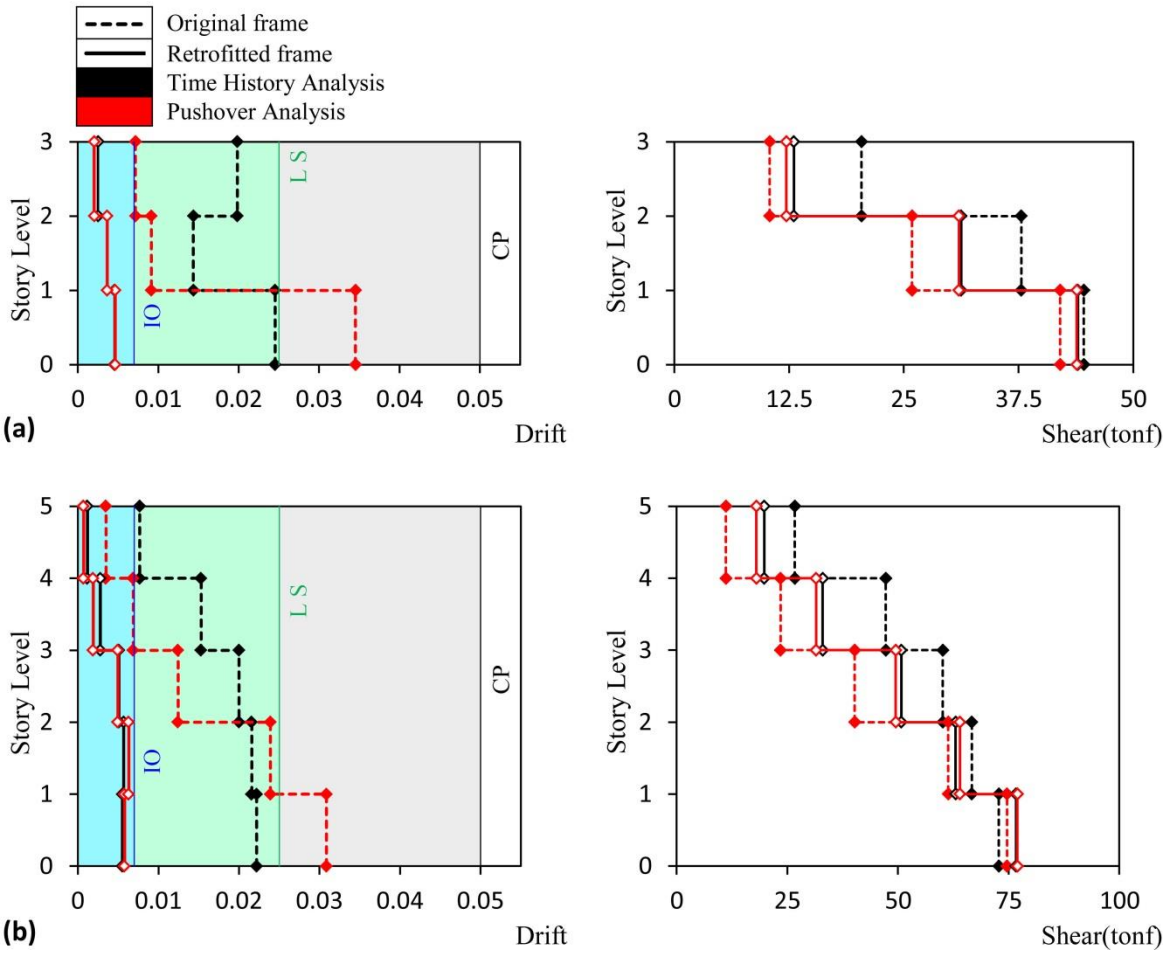

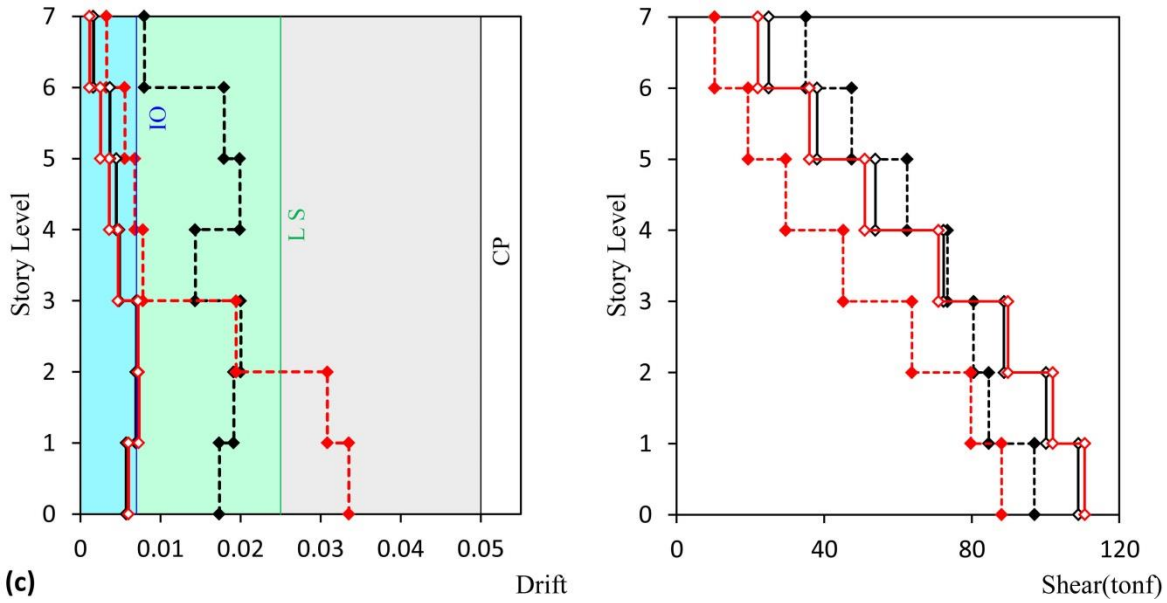

Figure 13- Comparison of the inter-storey drift ratios and storey shear forces obtained from the NTHA and pushover analyses at the DBE hazard level for (a) the 3-Storey, (b) 5-Storey and (c) 7-Storey bare frame and retrofitted case study buildings

3.3. Incremental Dynamic Analysis (IDA)

The Incremental dynamic analysis (IDA) comprehensively evaluates the performance of structures under various scaled earthquake records using a series of nonlinear dynamic analyses. In this method, the seismic demand and capacity of the structure can be properly estimated by covering a broad range of behaviour from elastic response to failure [47]. Currently, this method of analysis is considered as one of the best approaches for the reliability analysis and for the development of the fragility curves. In this study, the IDA are performed on the 3-Storey, 5-Storey and 7-Storey bare frame and retrofitted case study buildings to develop fragility curves for these structures.

The sufficient number of accelerograms needs to be used in the IDA to reduce uncertainties associated with the earthquake characteristics (i.e. aleatory uncertainty). Considering different sources of uncertainties, previous studies by Shome and Cornell [48] indicated that generally a minimum number of 10 incremental dynamic analyses is required to estimate the seismic demand and demand-hazard of non-linear systems with a good level of accuracy. Therefore, to reduce the earthquake input uncertainties, twelve far-field earthquake records were used to perform the incremental dynamic analyses in the current study as listed in Table 5. For each recorded earthquake, the horizontal component which has higher spectral acceleration value corresponding to the fundamental period of the selected buildings is used in the IDA analyses as the main record (see Table 5). This procedure is considered to be more accurate compared to the case that only the PGA of each horizontal component is considered.

To develop the IDA curves, in this work, the peak ground acceleration (PGA) is considered as the intensity measure (IM) and the maximum inter-storey drift is taken as the damage measure parameter (DM). Therefore, the IDA curves, which illustrate the correlation between DMs and IMs, are presented in the form of PGA vs drift. It should be noted that since the proposed retrofitting method can significantly influence the dynamic characteristics of the structures (see Table 4), in this study PGA is selected as a structurally independent intensity measure to provide a fair comparison between the response of the systems before and after retrofitting. Figure 14 shows the IDA Curves for the 3-Storey, 5-Storey and 7-Storey bare frame and retrofitted case study buildings along with the drift limits corresponding to performance levels given in

ASCE/SEI 41-17 [40]. The mean PGA values corresponding to the drift values at each limit state for the bare frame and retrofitted case study buildings are presented in Table 6.

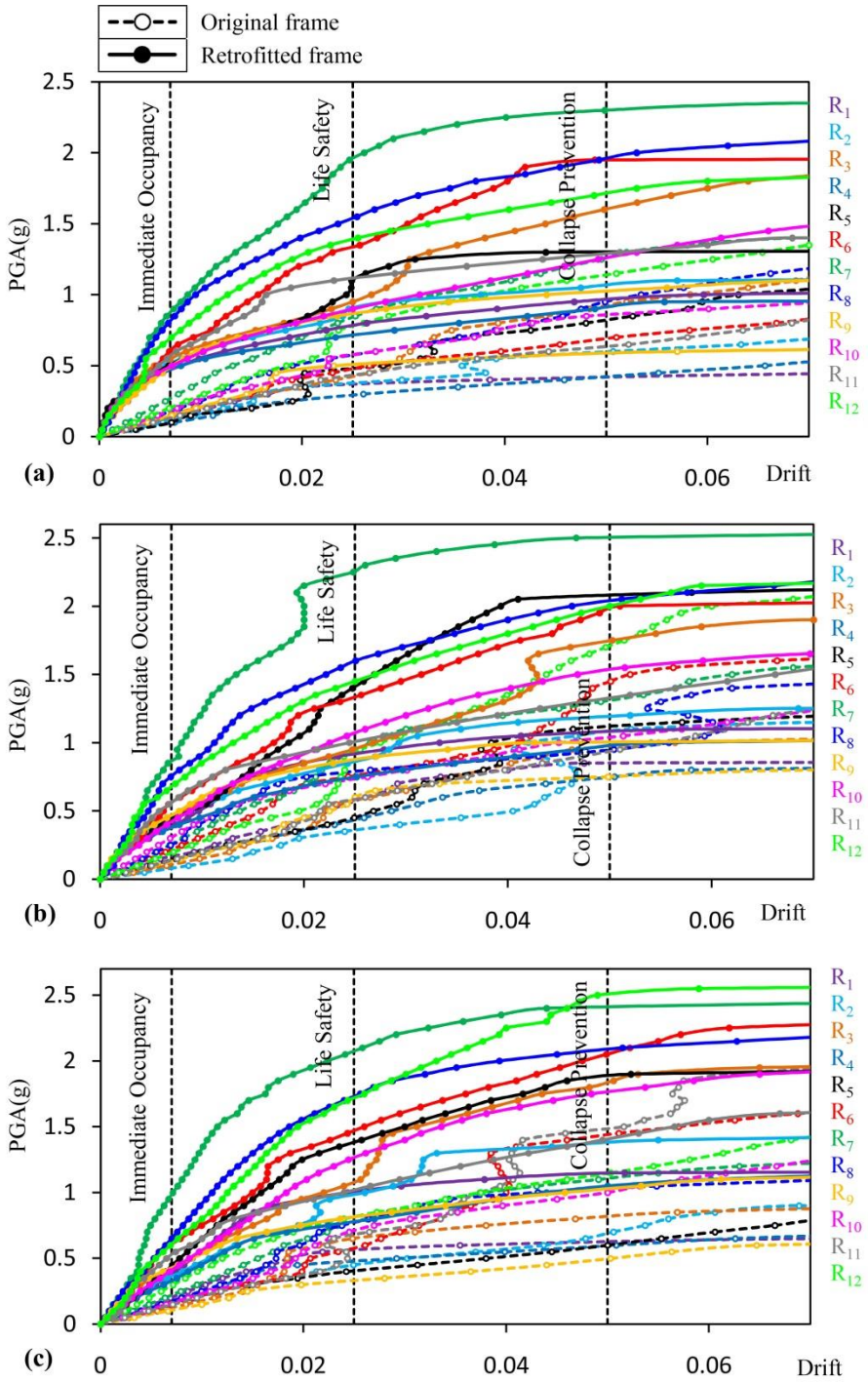

Figure 14- IDA Curves for (a) the 3-Storey, (b) 5-Storey and (c) 7-Storey bare frame and retrofitted case study buildings

The IDA results indicate that the proposed retrofitting method significantly enhance the intensity measure corresponding to different levels of performance. The PGA levels associated with IO performance level for the bare frame case study buildings are at least three times higher than those for the retrofitted case study buildings. For the retrofitted buildings, the drift values corresponding to IO performance level are approximately 1.5 times higher than the drift values corresponding to DBE (i.e. 0.35g). These ratios are around 2 and 1.5 for the LS and CP performance levels. These results verify the good performance of the retrofitted case study buildings; the buildings mainly work in the elastic range under strong ground motion conditions.

Table 6- Mean PGA values corresponding to the drift values at each limit state for (a) the 3-Storey, (b) 5-Storey and (c) 7-Storey bare frame and retrofitted case study buildings

Performance Levels	3-Storey Building		5-Storey Building		7-Storey Building	
	Bare Frame	Retrofitted	Bare Frame	Retrofitted	Bare Frame	Retrofitted
	PGA (g)					
IO	0.16	0.59	0.18	0.54	0.17	0.51
LS	0.51	1.13	0.65	1.21	0.60	1.28
CP	0.77	1.45	1.07	1.62	0.92	1.71

3.4. Fragility Analysis

For the assessment of the seismic response of structures, the most rational approach would be to utilize fragility curves and probabilistic analysis due to the wide range of aleatory and epistemic uncertainties [49]. The fragility curves represent the probability of exceeding different performance levels at a given level of ground motion and are defined with the following equation:

$$Fragility = P[R > LS_i | IM = S] \quad (6)$$

where R, LS_i, IM and S denote the structural response, limit state corresponding to R, intensity measure, and the realization of the intensity measure, respectively.

In general, the fragility curves represent the cumulative probability distribution of a damage measure (DM) as a function of an intensity measure (IM), using probabilistic analyses approach [50]. In this respect, whenever a specific level of intensity is of interest, the probability of exceeding the values corresponding to different performance levels can be expressed by extracting the distribution function for the responses (EDP-Based) [51]. In this study, to evaluate the seismic reliability of the proposed method of retrofitting, the fragility curves using the IDA method for constant performance levels have been obtained (IM-Based). First, the maximum values of acceleration associated with a specific level of performance are selected from the resulted IDA curves (see Figure 14). Subsequently, assuming a lognormal distribution for the captured values, a probability density function (F(x)) is extracted by computing the mean (μ) and standard deviation (δ) parameters in this damage level. According to Figure 15, when a value for "X_0" is considered as a certain level of intensity, the area under the probability density function from "-∞" to "X_0", demonstrates the structure's fragility. This means that at this level of intensity, the structure will experience the considered performance level with a probability of P [19]. Consequently, conforming to the rule of subtraction, "1-P" presents the structure's reliability for not reaching the above mentioned performance level under the given level of intensity (X_0).

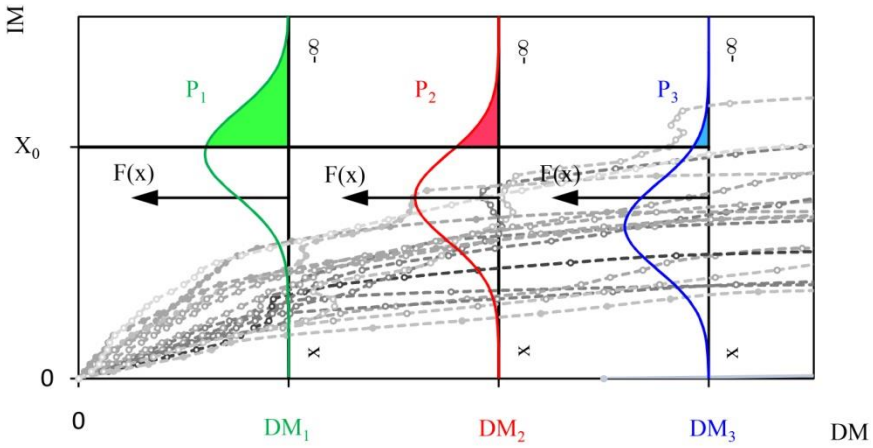

Figure 15- Probability of exceeding (P) a certain Performance Level at "X_0" Hazard Level (schematic)

In this work, the seismic fragility analysis of bare frame and retrofitted case study structures is performed based on the explained approach using the IDA results. From each IDA curve, PGAs values corresponding to the performance levels are identified for the bare frame and retrofitted buildings separately. For each performance level, mean and standard deviation of the PGA values are obtained for the bare frame and retrofitted buildings. Then, assuming a lognormal distribution, cumulative distribution functions are derived for each performance level for the bare frame and retrofitted buildings separately. Fragility curves for the structures under consideration are presented in Figure 16. As one can observe from this figure, the proposed retrofitting system highly reduces the fragility of the bare frame buildings. For the DBE and MCE, the probabilities of exceeding the performance levels are given in Tables 7 and 8, respectively. All these results indicate the efficiency of the vertical links to successfully retrofit the deficient SMRF systems.

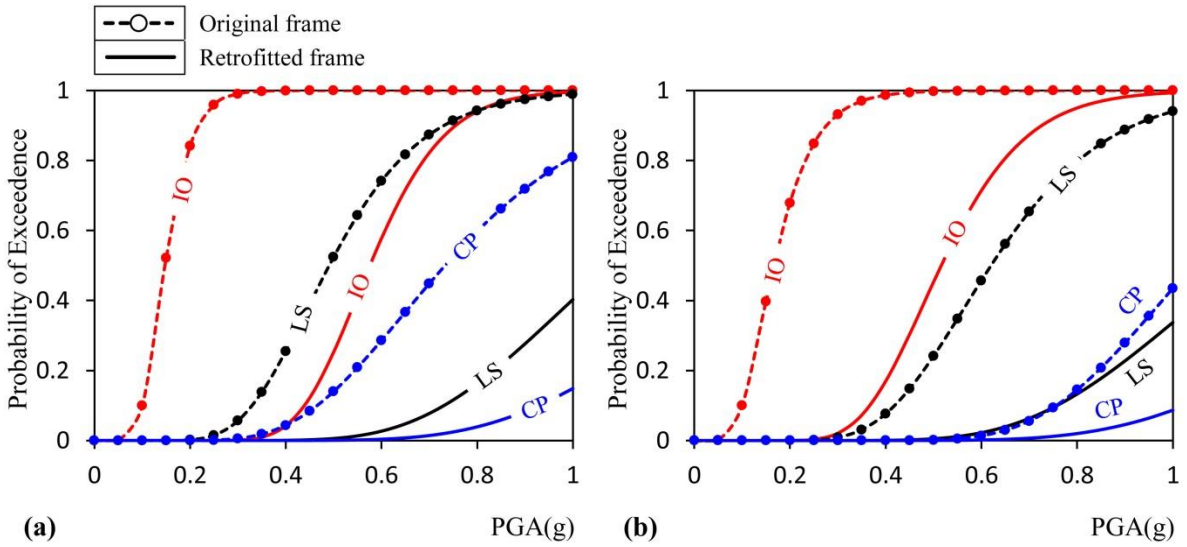

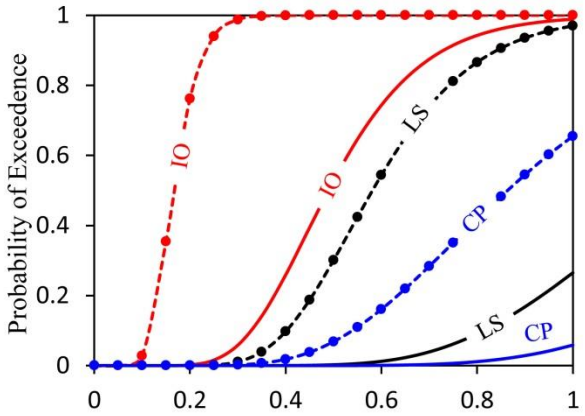

(c)

Figure 16- Fragility Curves for (a) the 3-Storey, (b) 5-Storey and (c) 7-Storey bare frame and retrofitted case study buildings

Table 7- Probability of exceeding different limit states under the earthquake intensities corresponding to the DBE (0.35g)

Performance Levels	3-Storey Building		5-Storey Building		7-Storey Building	
	Bare Frame	Retrofitted	Bare Frame	Retrofitted	Bare Frame	Retrofitted
	Probability of Exceedance (%)					
IO	99.77	0.94	96.96	7.25	99.76	14.13
LS	13.84	0.01	3.1	0.01	3.93	0
CP	1.84	0	0	0	0.70	0

Table 8- Probability of exceeding different limit states under the earthquake intensities corresponding to the MCE (0.55g) hazard level

Performance Levels	3-Storey Building		5-Storey Building		7-Storey Building	
	Bare Frame	Retrofitted	Bare Frame	Retrofitted	Bare Frame	Retrofitted
	Probability of Exceedance					
IO	99.99	41.47	99.87	59.43	99.99	64.61
LS	64.40	1.32	34.77	1.14	42.38	0.57
CP	20.87	0.15	0.52	0.06	10.96	0.03

As it can be observed, the application of the proposed method of retrofitting when the structures are subjected to the DBE, has led to the reliability of 99%, 93% and 86% for the 3, 5 and 7-storey frames in case of the performance level of IO. This implies that by means of this method, the reliability raises by 99, 90 and

85% compared to the original structure. Under this level of intensity, the reliability for lower level of performance in all retrofitted structures, is approximately 100%.

Moreover, in the event of MCE hazard level, if the performance level of IO is of concern, retrofitting manages to rate the reliability of the 3, 5 and 7-storey structures to 58%, 40% and 35%, respectively whereas reliability of the original structures for the mentioned level of performance under the MCE intensity has been less than 0.5%. Under the same level of intensity, reliability of all frames for lower levels of performance is greater than 98%.

Based on the results, this method of retrofitting, acts most effectively on the shorter structures and high levels of performance which could be attributed to the greater elastic stiffness of the shorter structures and effective role of the vertical links in providing this type of stiffness (see Figure 12).

It is worth noting that the observations and results obtained in this paper are limited to the assumptions and analyses conducted in this work. Therefore, the values that are reported in this work are indicative and cannot be taken as typical values. On the other hand, general conclusions that are also supported by the previous works can be drawn from the results of the numerical analysis in this study.

5. Conclusions

In this work, a series of NSA, NTHA and IDA are carried out on the bare frame and retrofitted SMRF buildings with WCSB to demonstrate the efficiency of eccentric bracing systems with vertical links as a seismic retrofitting technique. NSA and NTHA results are used to assess the performance of the retrofitted buildings in detail. IDA results are utilized to develop the seismic fragility curves for the retrofitted SMRF systems. Based on the analyses performed in this paper, the following conclusions are drawn:

1) The use of EBF with vertical links shortens the period of the first translational mode of the bare frame 3, 5 and 7-storey case study buildings by 62.5%, 61.16% and 56.7%, respectively. On the contrary, the increase in the translational effective mass participation factor for the first mode reduces the effect of links on the higher modes.

2) The height-wise distribution of earthquake loads for the retrofitted buildings fits an inverted triangular load distribution pattern better than that of for the bare frame case study buildings. A good agreement is observed between the results of NSA and NTHA results after retrofitting the case study buildings. Therefore, NSA can be used with high confidence for seismic analysis of the EBF systems with vertical links.

3) The eccentric bracing systems with vertical links improve the energy dissipation capacity, initial stiffness and load-carrying capacity of the SMRF systems with WCSB. For instance, after retrofitting, the target displacement of the frames remarkably reduces and higher performance levels are achieved under the DBE. The damage concentrates only on the vertical links for the DBE and the remaining structural members work in the elastic range as aimed in the design stage. The compression-induced buckling in the braces is alleviated.

4) The initial parts of capacity curves of the retrofitted case study buildings have two successive slopes. This implies a dual load-carrying system with varying levels of ductility and multi-level energy absorption capabilities. Obviously, these capabilities are very desirable for the structures built in earthquake-prone areas.

5) The PGA values corresponding to the IO performance level for the retrofitted structures, are around 3 times higher than those for the bare frame case study buildings. In contrast to the bare frames, the drift values for the retrofitted buildings corresponding to IO performance level are approximately 1.5 times higher than the drift values corresponding to DBE (i.e. 0.35g).

6) The probabilistic investigations indicate that the proposed retrofitting method considerably improves the seismic reliability of the case study buildings at different performance levels under the DBE. Accordingly, under this earthquake severity, the proposed retrofitting method enhances the reliability of the 3-Storey, 5-Storey and 7-Storey retrofitted case study buildings by 99%, 90% and 85%, respectively, at the IO performance level.

References

[1] Iranian Code of Practice for Seismic Resistant Design of Buildings, Permanent Committee for Revising the Standard 2800, 1st Edition, Building and Housing Research Center, Tehran, Iran, (1988).

[2] Iranian Code of Practice for Seismic Resistant Design of Buildings, Permanent Committee for Revising the Standard 2800, 4th Edition, Building and Housing Research Center, Tehran, Iran, (2014).

[3] Roeder CW, Popov EP, “Eccentrically braced steel frames for earthquake”, J Struct Div, ASCE;104(ST3) (1978a), pp.391–412.

[4] Schmidt K, Dorka UE, Taucer F and Magonette G, “Seismic retrofit of a steel frame and a RC frame with HYDE systems”, Report No. EUR 21180 EN, European Laboratory for Structural Assessment (ELSA), (2004).

[5] Roeder CW and Popov EP, “Inelastic behavior of eccentrically braced steel frames under cyclic loading”, University of California, Berkeley, UCB/EERC-77/18, (1977).

[6] Roeder CW and Popov EP, “Cyclic shear yielding of wide-flange beams”, J. Eng. Mech. Div. ASCE 104 (4), (1978b), pp. 763–780.

[7] Kasai I and Popov EP, "A study of seismically resistant eccentrically braced steel frame systems", Report No. UCB/EERC-83/15, Earthquake Engineering Research Center, Berkeley, CA, (1983).

[8] Hjelmstad KD and Popov EP, “Seismic behavior of active beam link in eccentrically braced frames”, Earthquake Engineering Research Center, University of California, Berkeley, CA, Report No. UCB/EERC-83/15, (1983a).

[9] Hjelmstad KD and Popov EP, “Cyclic behavior and design of link beams”, J. Struct. Eng. ASCE 109 (10), (1983b), pp. 2387–2403,.

[10] Hjelmstad KD and Popov EP, "Seismic behavior of active beam links in eccentrically braced frames", Report No. UCB/EERC-86/01, Earthquake Engineering Research Center, Berkeley, CA, (1986).

[11] Engelhardt MD and Popov EP, "Behavior of long links in eccentrically braced frames", Report No. UCB/EERC-89/01, Earthquake Engineering Research Center, Berkeley, CA, (1989).

[12] Engelhardt MD and Popov EP, “Experimental performance of long links in eccentrically braced frames”, J. Struct. Eng. ASCE 118 (11), (1992), pp. 3067–3088.

[13] ANSI/AISC 341-16, Seismic Provisions for Structural Steel Buildings, American Institute of Steel Construction, Chicago, IL, (2016).

[14] Ghobarah A and Ramadan T, “Seismic analysis of links of various lengths in eccentrically braced frames”, Can. J. Civ. Eng. 18 (1), (1991), pp.140–148,.

[15] Daneshmand A and Hashemi BH, “Performance of intermediate and long links in eccentrically braced frames”, J. Constr. Steel Res. 70, (2012), pp. 167–176.

[16] ANSI/AISC 360-10, Specification for Structural Steel Buildings, American Institute of Steel Construction, Chicago, IL, (2010).

[17] Seki M, Katsumata H, Uchida H and Takeda T, "Study on earthquake response of two-storied steel frame with y-shaped braces", Proceedings 9th World Conference on Earthquake Engineering, Tokyo-Kyoto, Japan, (1988), pp. 65-70.

[18] Baradaran MR, Hamzezarghani F, Rastegari G. M. and Mirsanjari Z, "The effect of vertical shear-link in improving the seismic performance of structures with eccentrically bracing systems", International Journal of Civil and Environmental Engineering, Vol. 9, No. 8, (2015), pp. 1078-1082.

[19] Mohsenian V and Mortezaei A, "Evaluation of seismic reliability and multi level response reduction factor (R factor) for eccentric braced frames with vertical links", Earthquakes and Structures, 14(6), (2018a) pp. 537-549.

[20] Mohsenian V and Mortezaei A, "A new energy-absorbing system for seismic retrofitting of frame structures with slender braces", Bulletin of Earthquake Engineering, DOI: https://doi.org/10.1007/s10518-018-00543-7, (2018b).

[21] Zahrai SM and Moslehi Tabar A, "Analytical study on cyclic behavior of chevron braced frames with shear panel system considering post-yield deformation", Canadian Journal of Civil Engineering, Vol. 40, No. 7, (2013), pp. 633-643.

[22] Sabouri-Ghomi S and Saadati B, "Numerical modeling of links behavior in eccentric bracings with dual vertical links", Numerical Methods in Civil Engineering, 1(1), (2014), pp.14-20.

[23] Zahrai SM and Parsa A, "Effect of flange width of vertical link beam on cyclic behavior of chevron braced steel frames", Journal of Seismology and Earthquake Engineering, Vol. 17, No. 4, (2015), pp. 281-292.

[24] Lian M and Su M, "Seismic performance of high-strength steel fabricated eccentrically braced frame with vertical shear link", Journal of Constructional Steel Research, Vol. 137, (2017), pp. 262-285.

[25] Daryan A, Bahrampoor H, Ziaei M, Golafshar A and Assareh, MA, "Seismic behavior of vertical shear links made of easy-going steel", American Journal of Engineering and Applied Sciences, 1(4), (2008) pp. 368-377.

[26] Duan L and Su M, "Seismic testing of high-strength steel eccentrically braced frames with a vertical link", Proceedings of the Institution of Civil Engineers-Structures and Buildings, Vol. 170, Issue 11, (2017), pp. 874-882.

[27] Massah SR and Dorvar H, "Design and analysis of eccentrically braced steel frames with vertical links using shape memory alloys", Smart Materials and Strucrures, 23, (2014), DOI:10.1088/0964-1726/23/11/115015.

[28] Shayanfar MA, Barkhordari MA and Rezaeian AR, "Experimental study of cyclic behavior of composite vertical link in eccentrically braced frames", Steel and Composite Structures, Vol. 12, No. 1, (2012), pp. 13-29.

[29] Bouwkamp J, Vetr MG and Ghamari A, "An analytical model for inelastic cyclic response of eccentrically braced frame with vertical shear link (V-EBF)", Case Studies in Structural Engineering, Vol. 6, (2016), pp. 31-44.

[30] Vetr MG, Ghamari A and Bouwkamp J, "Investigating the nonlinear behavior of eccentrically braced frame with vertical shear links (V-EBF)", Journal of Building Engineering, Vol. 10, (2017), pp. 47-59.

[31] Fehling E, Pauli W and Bouwkamp JG, "Use of vertical shear-links in eccentrically braced frames", Proceedings of the 10th World Conference on Earthquake Engineering, Rotterdam, The Netherlands, (1992), pp. 4475–4480.

[32] Shayanfar MA, Rezaeian AR and Taherkhani S, "Assessment of the seismic behavior of eccentrically braced frame with double vertical link (dv-ebf)", Proceedings of the 14th World Conference on Earthquake Engineering, October 12-17, Beijing, China, (2008).

[33] Rahnavard R, Hassanipour A, Suleiman M and Mokhtati A, "Evaluation on eccentrically braced frame with single and double shear panels", Journal of Building Engineering, Vol. 10, (2017), pp. 13-25.

[34] Shayanfar MA and Rezaeian AR, "Assessment of seismic behavior of eccentrically braced frame with double vertical link (DV-EBF)", Proceedings of the 3rd International Conference on Advances in Experimental Structural Engineering, San Francisco, CA, (2009).

[35] Zahrai SM and Mahroozadeh Y, "Experimental study of using vertical link beam to improve seismic performance of steel buildings", Journal of Civil and Surveying Engineering, Vol. 44, Issue. 3, (2010), pp. 379-393.

[36] Mohsenian V, Nikkhoo A, "Evaluation of performance and seismic parameters of eccentrically braced frames equipped with dual vertical links", Structural Engineering and Mechanics, 69(6), (2019), pp. 591-605.

[37] ASCE/SEI 7-10, Minimum Design Loads and Associated Criteria for Buildings and Other Structures, American Society of Civil Engineers, Reston, Virginia, (2010).

[38] Elkady A, Lignos DG, "Modeling of the composite action in fully restrained beam-to-column connections: implications in the seismic design and collapse capacity of steel special moment frames", Earthquake Engineering and Structural Dynamics, Vol. 43, No. 13, (2014), pp. 1935-1954.

[39] PERFORM-3D Nonlinear Analysis and Performance Assessment for 3D Structures, CSI-Computers and Structures Inc., Version 6.0.0, Berkeley, CA, USA, (2016).

[40] ASCE/SEI 41-17, Seismic Evaluation and Retrofit of Existing Buildings, ASCE Standard 41, Published by The American Society of Civil Engineers, Reston, Virginia, USA, (2017).

[41] Lignos DG, Krawinkler H, "Deterioration modeling of steel components in support of collapse prediction of steel moment frames under earthquake loading", Journal of Structural Engineering, Vol. 137, No. 11, (2010), pp. 1291-1302.

[42] ABAQUS Users Manual, Version 6.14, SIMULIA World Headquarters. Rissing Sun Mills 166 Valley Street, Providence (RI 02909-2499, USA), (2014).

[43] PEER Ground Motion Database, Pacific Earthquake Engineering Research Center, Web Site: http:// peer.berkeley.edu/peer-ground-motion-database, Accessed on Feb 15, (2019).

[44] Baker JW, "Conditional Mean Spectrum: Tool for Ground-Motion Selection", Journal of Structural Engineering, 137 (3), (2011), pp. 322-331.

[45] Haselton CB, Whittaker AS, Hortacsu A, Baker JW, Bray J, Grant DN. "Selecting and Scaling Earthquake Ground Motions for Performing Response-History Analyses", 15WCEE, Lisbon, Portugal, (2012).

[46] Hancock J, Watson-Lamprey J, Abrahamson NA, Bommer JJ, Markatis A, McCoy E and Mendis R "An improved method of matching response spectra of recorded earthquake ground motion using wavelets ", Journal of Earthquake Engineering, 10, (2006), pp.67-89.

[47] Vamvatsikos D and Cornell CA, "Incremental dynamic analysis", Earthquake Engineering Structural Dynamics, 31(3), (2002), pp.491-514.

[48] Shome N and Cornell CA, "Probabilistic seismic demand analysis of nonlinear structures", Reliability of Marine Structures Report No: RMS-35, Civil and Environmental Engineering, Stanford University, (1999).

[49] Ang AHS and Tang WH, "Probability concepts in engineering: emphasis on applications to civil and environmental engineering", 1, Wiley, 2nd Edition, the University of Michigan, (2007).

[50] Cimellaro GP, Reinhorn AM, Bruneau M and Rutenberg A, “Multi-dimensional fragility of structures: formulation and evaluation”, Technical Report MCEER-06-0002, (2006).

[51] Zareian F, Krawinkler H, Ibarra L and Lignos D, “Basic concepts and performance measures in prediction of collapse of buildings under earthquake ground motions”, The Structural Design of Tall and Special Buildings, 19, (2010), pp.167-181, DIO: 10.1002/tal.546.